J | P | S | T

http://jpst.irost.ir

Journal of Particle Science and Technology

IROST

Numerical simulation of nanofluids flow and heat transfer through isosceles triangular channels

Mehri Hejri[1], Mohammad Hojjat[2,*], Seyed Gholamreza Etemad[3,4]

[1] *Department of Chemical Engineering, Quchan Branch, Islamic Azad University, Quchan, Iran*

[2] *Department of Chemical Engineering, Faculty of Engineering, University of Isfahan, Isfahan, Iran*

[3] *Department of Chemical Engineering, Isfahan University of Technology, Isfahan, Iran*

[4] *International Academy of Science, Engineering, and Technology, Ottawa, Canada*

HIGHLIGHTS

- Laminar heat transfer nanofluid inside an isosceles triangle cross section is investigated.
- Higher volume concentration is conducive to heat transfer.
- Increased nanoparticle concentration increases the pumping power.
- Increasing the apex angle of the channels decreases the friction coefficient and pressure drop.

GRAPHICAL ABSTRACT

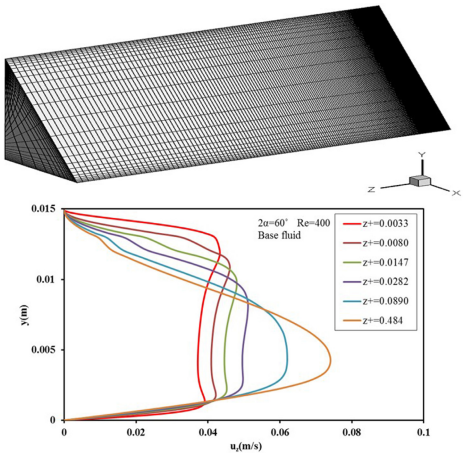

ARTICLE INFO

Article history:

Received 13 May 2018
Revised 10 July 2018
Accepted 13 July 2018

Keywords:

Nanofluids
Hear transfer coefficient
Nusselt number
Numerical simulation
Triangular duct

ABSTRACT

Nanofluids are stable suspensions of nanoparticles in conventional heat transfer fluids (base fluids) that exhibit better thermal characteristics compared to those of the base fluids. It is important to clarify various aspects of nanofluids behavior. In order to identify the thermal and hydrodynamic behavior of nanofluids flowing through non-circular ducts, in the present study the laminar flow forced convective heat transfer of Al_2O_3/water nanofluid thorough channels with isosceles triangle cross section with constant wall heat flux was studied numerically. The effects of nanoparticle concentration, nanofluid flow rate and geometry of channels on the thermal and hydrodynamic behavior of nanofluids were studied. The single-phase model was used in simulations under steady state conditions. Results reveal that the local and average heat transfer coefficients of nanofluids are greater than those of the base fluid. Heat transfer coefficient enhancement of nanofluids increases with increase in nanoparticle concentration and Reynolds number. The local heat transfer coefficient of the base fluid and that of the nanofluids decrease with the axial distance from the channel inlet. Results also indicate that an increase in the apex angle of the channel, decreases the Nusselt number and heat transfer coefficient. The wall friction coefficient decreases with increasing axial distance from the channel inlet and approaches a constant value in the developed region. Friction coefficient and pressure drop decrease by increasing the apex angle of the channels.

** Corresponding author: Tel.: +9831-37934074 ; Fax: +9831-37934031 ; E-mail address: m.hojjat@eng.ui.ac.ir*

DOI: 10.22104/JPST.2018.2905.1124

1. Introduction

Since heat transfer has widespread applications in various industries, enhancement of the efficiency of heat transfer equipment has become a priority for industrial designers and researchers. The efforts of scientists in this regard have led to the invention of many different techniques. Two of these methods that have been used in the present study are the use of non-circular channels and the use of nanofluids as a new class of heat transfer fluids. Utilization of non-circular flow passage geometries is required, particularly in construction of compact heat exchangers, because of the size and volume constraints in heat transfer applications such as aerospace, biomedical engineering and electronics. Relatively low thermal characteristics of heat transfer fluids, such as water, engine oil and ethylene glycol, are limiting factors in the improvement of the efficiency of heat transfer devices. Solids have large thermal conductivity; therefore, it seems that dispersion of solid particles in fluids may improve their thermal characteristics [1]. Many investigations have been made on the thermal behaviour of nanofluids using computational fluid dynamics (CFD). Investigations have been conducted considering mixed and forced convective heat transfer in laminar and turbulent flow regimes. The simulation can be performed using a single phase model or a two-phase model. In the single phase model, nanoparticles and base fluid behave as a homogeneous fluid. This requires less computational time in comparison to a two-phase model. Lotfi *et al.* compared these two approaches for nanofluids flowing in a circular tube in a laminar regime [2]. Their results show that the mixture model is a more precise model. They illustrated that the single-phase model and the two-phase Eulerian model underestimate the Nusselt number. A similar study was also conducted by Saberi *et al.* on a vertical tube [3]. According to their results, the mixture model has better agreement with experimental data, while the prediction of nanofluid mean bulk temperature distribution inside the tube by the single phase model is better than the mixture model. Bianco *et al.* and Nazififard *et al.* investigated the turbulent flow convective heat transfer of nanofluids [4-6]. Their results show that heat transfer increases by increasing the nanoparticle volume concentration and Reynolds number. Rostamani *et al.* have numerically analyzed the turbulent flow of nanofluids with different concentrations through a two dimensional duct [7]. Their results are similar to those of Bianco and Nazififard [6]. They also analyzed the effect of nanoparticles type on heat transfer. They found that for a constant volume concentration and Reynolds number, the effects of CuO nanoparticles on the heat transfer enhancement is more than those of Al_2O_3 and TiO_2 nanoparticles. Laminar flow heat transfer of nanofluids flowing in an isosceles triangular duct with constant wall temperature was simulated numerically [8]. Results show that the heat transfer coefficient and the Nusselt number of nanofluids is enhanced by increasing the nanoparticle concentration and Peclet number. Convective heat transfer of nanofluids through different geometrical configurations including horizontal straight circular tubes [9-16], vertical circular tube [3], annulus [17], elliptic ducts [18], square ducts [19-25], rectangular ducts [26], and triangular ducts [8, 23,27-31] have been investigated.

In the present study, laminar flow forced convective heat transfer of Al_2O_3/water nanofluid thorough an isosceles triangular cross sectional channel with constant wall heat flux was simulated numerically. Simulations were carried out based on the single-phase model. The effects of parameters, such as nanoparticle concentration, flow rate of nanofluids and the geometry of channels on thermal and hydrodynamic behavior of nanofluids, were studied.

2. Problem statement

The geometry under consideration is shown in Figure 1a. Since the channel is geometrically symmetric, simulations have been performed for half of the channels (Figure 1b). Steady-state, laminar forced convective heat transfer of aqueous suspensions of Al_2O_3 nanoparticles with a diameter of 25 nm flowing through horizontal isosceles triangular ducts with apex angles of 60°, 90° subjected to constant wall heat flux were considered. Simulations have been made for nanofluids with concentrations of 0.1, 0.5, 1, 3, and 5 volume percent. It was assumed that there is no temperature and velocity differences between base fluid and nanoparticles, so single phase flow is used. The hydraulic diameter of all channels is considered to be 0.01m. The dimensions of channels, defined in Figure 1a, are calculated as:

$$D_h = \frac{4A}{P} \tag{1}$$

where A is the flow area and P is the wetted perimeter of the conduit.

$$D_h = \frac{4xy}{2(\sqrt{x^2+y^2}+x} \quad (2)$$

and

$$\tan\alpha = \frac{x}{y} \quad (3)$$

For a channel with given apex angle, x and y are calculated.

Non-uniform meshes were used. The number of grids were changed until increasing the grid number has any significant effect on the velocity, temperature and Nusselt number of fluids. The selected grid is presented in Table 1. Meshes are closer to each other near the walls and inlet of the channels because in these sections velocity and temperature gradients are more pronounced (Figure 1b). To investigate the effect of flow rate, simulation has been done at four different Reynolds numbers of 400, 800, 1200, and 1600.

Table 1. The selected grid for numerical simulation (x, y, s, and z are presented in Figure 1a).

2α	x	y	s	z
60	12	36	26	200
90	14	42	28	200

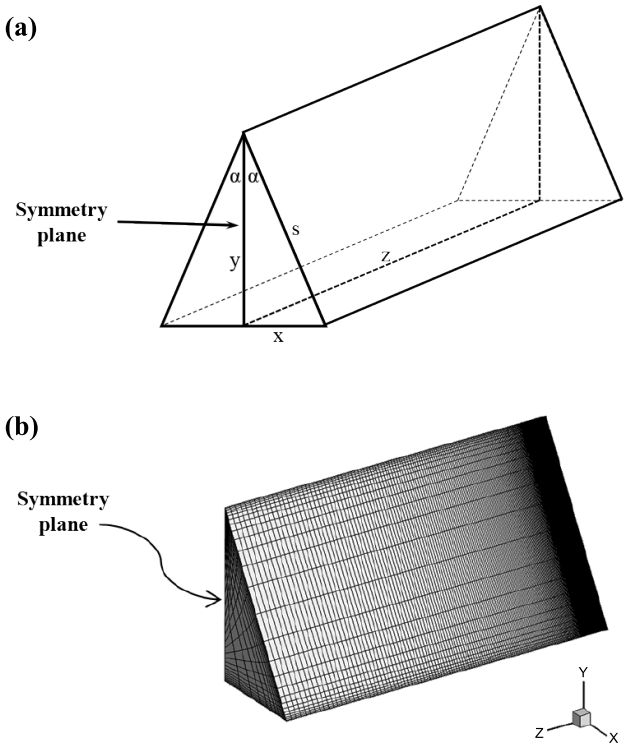

2.1. Governing equations

Hydrodynamic and thermal behavior of fluids through channels were obtained by solving continuity, momentum and energy equations in three dimensions for incompressible fluid as:

• Continuity equation

$$\nabla.(\rho_{eff} V)=0 \quad (4)$$

• Momentum equation

$$\nabla.(\rho_{eff}\nabla V) = -\nabla p + \nabla.(\mu_{eff}\nabla V) \quad (5)$$

• Energy equation

$$\nabla.(\rho_{eff} V C_{p,eff} T) = \nabla.(k_{eff}\nabla T) \quad (6)$$

The average heat transfer coefficient is calculated by Eq. (7), where N is the number of nodes in the axial direction and Δz_i is shown in Figure 2.

$$h = \frac{1}{L}\int h_z\, dz = \frac{1}{L}\sum_{i=1}^{N} h_{z_i}\Delta z_i \quad (7)$$

The average Nusselt number is calculated as follows:

$$Nu = \frac{hD_h}{k} \quad (8)$$

3. Physical properties of nanofluids

Thermophysical properties of nanofluids at the inlet temperature were obtained according to the following equations [12,13,32]:

$$\rho_{nf} = (1-\varphi)\rho_{bf} + \varphi\rho_{np} \quad (9)$$

$$C_{p_{nf}} = \frac{(1-\varphi)\rho_{bf}C_{p_{bf}} + \varphi\rho_{np}C_{p_{np}}}{\rho_{np}} \quad (10)$$

$$k_{nf} = k_{bf}(4.97\varphi^2 + 2.72\varphi + 1) \quad (11)$$

$$\mu_{nf} = \mu_{bf}(123\varphi^2 + 7.3\varphi + 1) \quad (12)$$

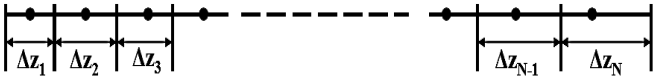

Fig. 2. Parameters of Eq. (7).

4. Boundary conditions

The governing equations were solved by considering the following boundary conditions:

• At the channel inlet (z = 0)

$V_z = V_0$, $V_x = V_y = 0$

$T = T_0$ (13)

• At the channel outlet (z = L)

Thermally and hydrodynamically developed conditions were considered.

• At the channel walls:

$V_x = V_y = V_z = 0$ (no slip condition) (14)

$q = q_w$ (constant wall heat flux)

5. Numerical procedure

Finite volume technique was used to solve the governing equations (Eqs. (4)-(6)). This method is based on the spatial integration of the governing equations over finite control volumes. A segregated formulation was adopted to solve the coupled conservation equations sequentially. The convective and the diffusive terms were discretized using the second order upwind method. Pressure-velocity coupling was achieved using the SIMPLE algorithm.

6. Results and discussion

6.1. Thermal behavior

In order to validate the accuracy of the present simulation, fully developed Nusselt numbers of water flowing through the triangular duct with different apex angles of 60° and 90° obtained from simulations were compared with the values reported by Shah and London [33]. The maximum and average differences between these values were 4.40% and 3.94%, respectively, which indicate the accuracy of the simulations.

Figure 3 shows the wall and bulk temperatures of the nanofluids as a function of axial distance for the duct with an apex angle of 60° at a Reynolds number of 400. It can be observed that an increase in nanoparticle concentration causes the wall temperature and the bulk temperature to decrease. This is the consequence of an increase in heat transfer coefficient of fluids due to the presence of nanoparticles. Wall temperature is influenced by nanoparticle concentration more than nanofluids bulk temperature. For example, the wall temperature of nanofluid with 5 vol% concentration is about 3.65% lower than that of the base fluid, while it is about 1.65% lower for fluid bulk temperature. This is in agreement with experimental results obtained by Zeinali Heris *et al.* [30].

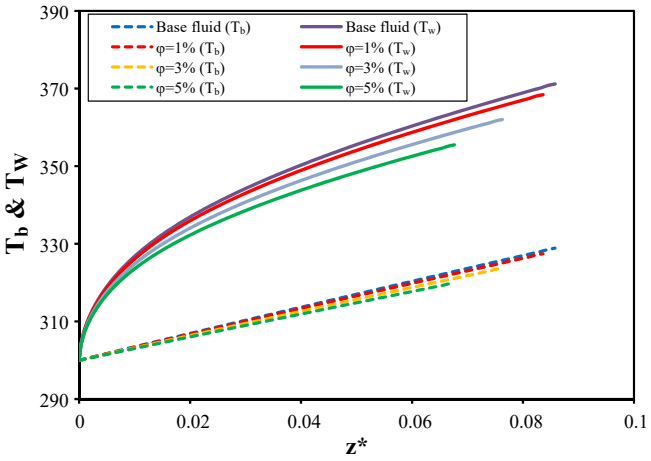

Fig. 3. Bulk and wall temperature vs. axial position for different nanoparticle concentrations.

Figure 4 shows the local heat transfer coefficient of nanofluids as a function of the axial distance for the duct with an apex angle of 60°. The local heat transfer coefficient of fluids decreases by increasing the axial distance from the duct entrance. This is due to the increase in the boundary layer thickness. The local heat transfer coefficient of nanofluids increases with an increase in nanoparticle concentration. This enhancement is larger at the entrance of the ducts. For instance, for the channel with an apex angle of 60°, increasing the nanoparticle concentration from 0% to 5% increases the local heat transfer coefficient about 32% at the entrance of channel, while at the fully developed region it increases about 15%. Similar trends were observed at other values of Reynolds numbers and for the channel with an apex angle of 90°. Improvement of thermal conductivity of nanofluids is the main factor that causes the convective heat transfer coefficient of nanofluids to increase. It also seems that the boundary layer of nanofluids grows slower than that of the base fluid and that the rate of growth decreases by increase in nanoparticle concentration, i.e. at a given distance from the duct inlet the boundary layer thickness of nanofluid is less than that of the base fluid. The local heat transfer coefficient, h, can be approximately

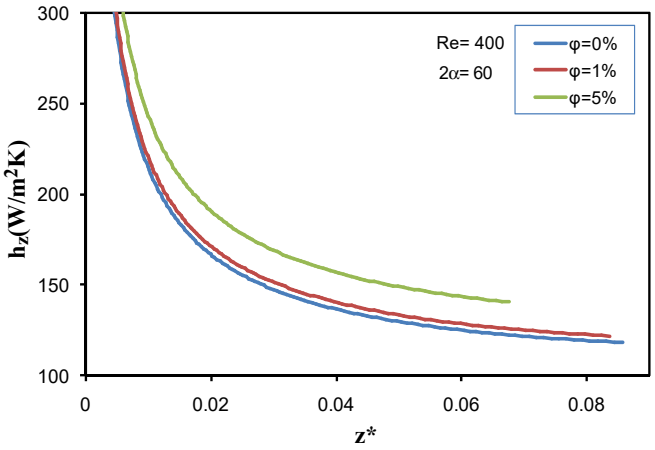

Fig. 4. Local heat transfer coefficient of nanofluids vs. axial position for different nanoparticle concentrations.

given as k/δt, where δt is the thickness of the thermal boundary layer [16]. Thus, the improvement of the heat transfer coefficient is due to the enhancement of thermal conductivity of nanofluids and also decreasing the thermal boundary layer thickness. This is in agreement with results obtained by Ghavam *et al.* [8].

Average heat transfer coefficient of nanofluids at different nanoparticle concentrations as a function of Pe, for two apex angles of 60° and 90° is shown in Figure 5. Heat transfer coefficient of nanofluids increases with an increase in the Peclet number, because the flow rate has a direct influence on the boundary layer thickness. The effect of the Peclet number on the heat transfer coefficient is the same for both the base fluid and nanofluids. However, the influence of the Peclet number on the heat transfer coefficient is more pronounced in the channel with a higher apex angel. When the Peclet number of 3 vol% nanofluid flowing through channels with apex angles of 60° and 90° changes from 2600 to 10500, the heat transfer coefficient enhances about 76 and 84 percent, respectively. This is in agreement with the results obtained by Ghavam *et al.* [8] for similar ducts with constant wall temperature. These results also indicate that the influence of flow rate on the enhancement of heat transfer coefficient is larger in the case of ducts that are subjected to constant wall heat flux.

Figure 6 indicates the effect of nanoparticle concentration and apex angle on average heat transfer coefficient. The value of h_{ave} increases with nanoparticle concentration. For example, the average heat transfer coefficient of nanofluids with a nanoparticle volume concentration of 5% is about 23%, and 24% greater than those of the base fluid for channels with apex angles of 60° and 90°, respectively. This indicates that the effect of nanoparticles on the heat transfer enhancement of both channels is almost the same. Similar results were obtained by Ghavam *et al.* [8].

The average Nusselt number of nanofluids as a function of nanoparticle concentration for channels with different apex angles at constant Reynolds number of 400 is shown in Figure 7. The Nusselt number of nanofluids also increases with an increase in nanoparticle concentration. For example, the average Nusselt numbers of nanofluid with 3% by volume concentration through the channels with apex angles of 60° and 90° are about 3.5 and 4 percent greater than those of the base fluid, respectively. Clearly, the enhancement of the average Nusselt number is less than that of the heat transfer coefficient. This is due to the fact that both the effective thermal conductivity and the heat transfer

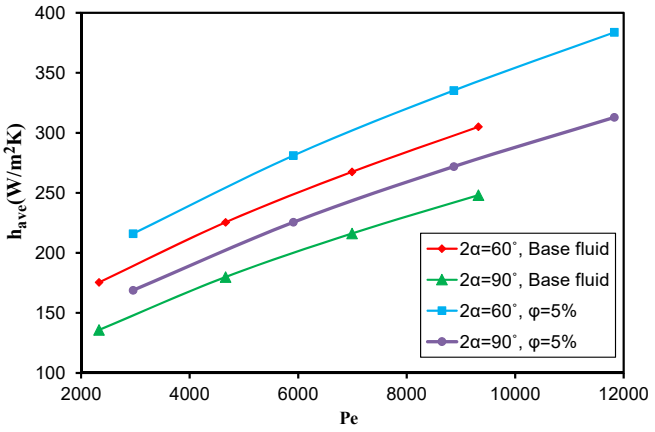

Fig. 5. Average heat transfer coefficient of nanofluids vs. Pe for different values of channel apex angle and different nanoparticle concentrations.

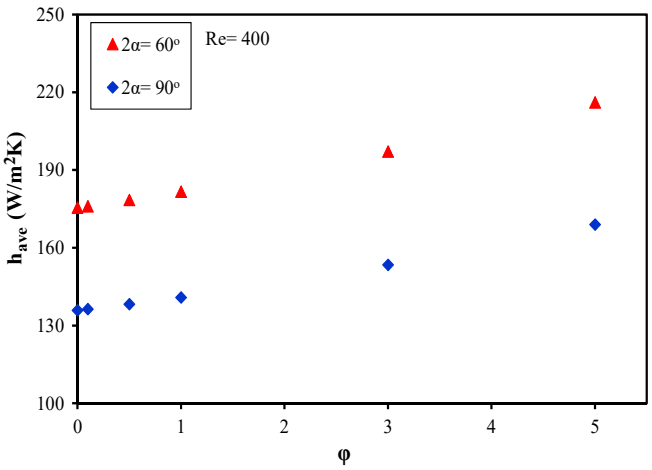

Fig. 6. Average heat transfer coefficient of nanofluids vs. nanoparticle concentration for channels with different apex angles.

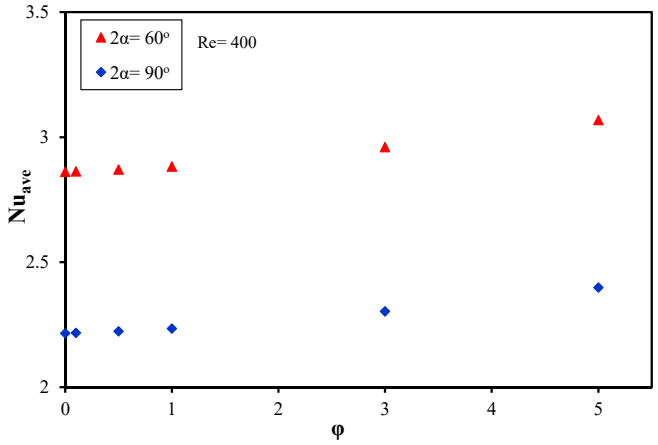

Fig. 7. Average Nusselt number vs. nanoparticle concentration for channels with different apex angles.

coefficient of the base fluid enhance as a results of adding nanoparticles. It is obvious that the improvement of the heat transfer coefficient is more than that of the thermal conductivity.

Laminar forced convection heat transfer of Al_2O_3/water nanofluids through an equilateral triangular duct was studied numerically using the dispersion model [27]. They used nanoparticles with 10, 20, 30, 40, and 50 nm diameters to identify the effect of particle size on thermal behavior of nanofluids. Their results show that the heat transfer coefficient of nanofluid is remarkably higher than that of the base fluid. The enhancement in heat transfer resultingfrom the present study is much less than those of their investigation. For example, their results show that the Nusselt number of nanofluids with 1% by volume of nanoparticles of 20 nm diameter at Re= 400 is about 10% higher than the base fluid, while the corresponding value obtained in the present study is about 1%. This is due to the difference in models used for these two studies and a difference between the sizes of nanoparticles.

6.2. Hydrodynamic behavior

Values of $f_{app}Re$ from the present study for water flowing through triangular ducts with an apex angles of 60° and 90° were compared with the values reported by Shah and London to validate the simulations [33]. Maximum and average differences between these values are 7% and 4.5%, respectively, which show the accuracy of the results.

Apparent Darcy friction factor, f_{app}, is defined as Eq. (15) [33].

$$f_{app} = \frac{4\Delta P/\rho u_m^2}{z/D_h} \tag{15}$$

Figure 8 indicates the $f_{app}Re$ of nanofluids as a function of the axial distance for the duct with an apex angle of 60°. The figure shows that $f_{app}Re$ decreases with axial distance and approaches to a constant value that is the fully developed value. According to the results obtaining from this figure, nanoparticle concentration has no significant effect on $f_{app}Re$.

The values of fully developed fRe for both channels are illustrated in Table 2. It is observed that the channels with a greater apex angle have a lower $f_{app}Re$ at the same Reynolds number.

The entrance length of channels with apex angles of 60 and 90 degrees are about L^+= 0.1 and 0.11, respectively, which are in agreement with previous proposed data [33,34]. Nanoparticle concentration has no significant effect on the entrance length. The dimensionless hydrodynamic entrance length (L^+) is defined as [34]:

$$L^+ = \frac{l}{D_h Re} \tag{16}$$

where l, the hydrodynamic entrance length, is defined as when the axial length of the duct which is required to achieve maximum axial velocity reaches within 99

Table 2. Fully developed values of fRe for two apex angles.

2α	Re			
	400	800	1200	1600
60	58.60	56.99	55.34	53.68
90	56.60	54.87	53.08	51.27

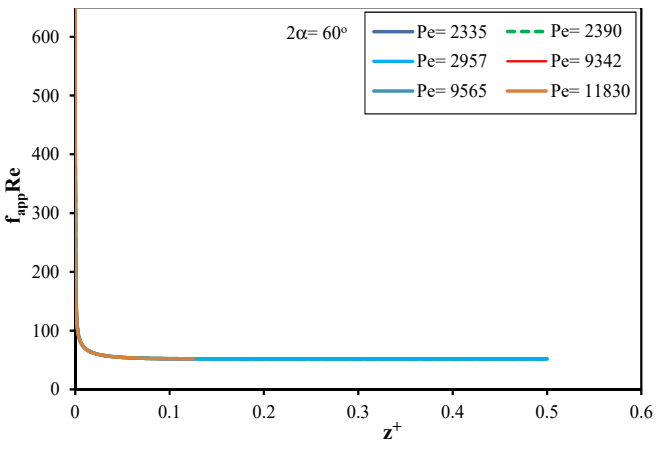

Fig. 8. The $f_{app}Re$ of nanofluids vs. axial position for different Peclet numbers.

percent of its fully developed value.

Figure 9 indicates the velocity profile of base fluid on the symmetry surface at different axial distance of the channels. It is clear that the flow is fully developed at the end of the channel. Similar results are obtained for nanofluids.

Figure 10 presents the axial velocity profiles of fluids on the symmetry surface at z^+=0.0033 (near the duct entrance) and near the end of the channels (fully developed condition). It is observed that at the entrance of the channels the velocity profiles of all fluids exhibit two local maxima near the walls. In order to satisfy no-slip condition the velocity of fluid at the walls reduces to zero by viscous friction, to satisfy the equation of continuity the velocity of fluid must increase in other sections. This increase in velocity cannot immediately reach the center, therefor for the small values of z, two local maxima appears in the velocity profile. By increase in axial distance from the duct inlet, the rise in axial velocity approaches the center of the duct and the velocity profile will have a maximum. It seems that the location of the maximums is independent of nanoparticle concentration, while the values of maximums is a function of nanofluid concentration [35].

The pumping power of nanofluids was calculated by Eq. (17) [36]:

$$\dot{W}_P = \frac{\dot{m}\Delta P}{\rho} \tag{17}$$

Figure 11 displays the effect of nanoparticle concentrations on the pumping power of fluids in the channels. The pumping power increases with the increase in nanoparticle concentration for both apex angles. According to the results, the pumping power is affected by the channel apex angle. The average required power for the channel with an apex angle of 90° is almost 12% greater than that of the channel with an apex angle of 60°.

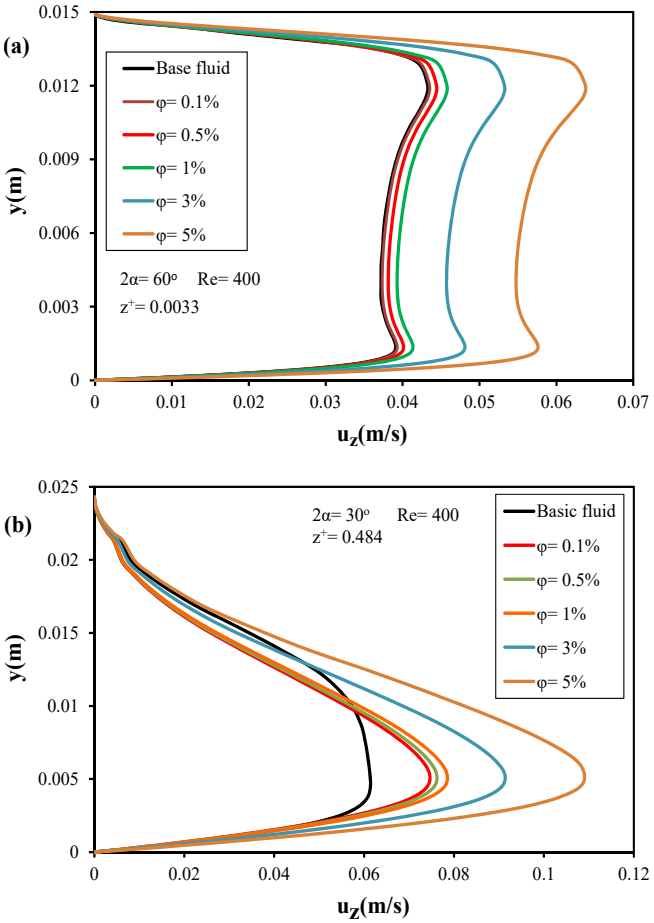

Fig. 10. The velocity profile of fluids on the symmetry surface at the entrance (a) and near the end (b) of the channels.

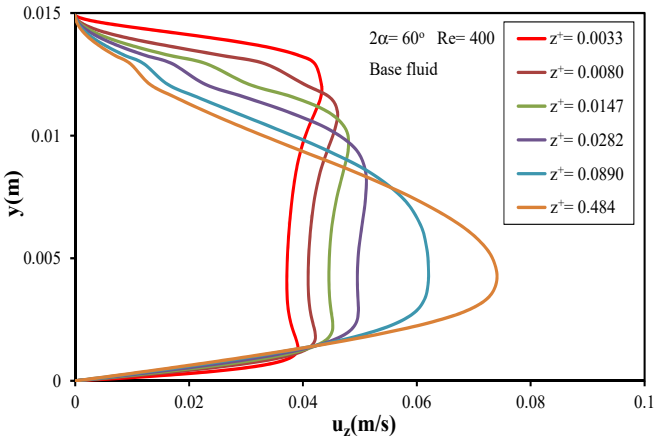

Fig. 9. The velocity profile of base fluid on the symmetry surface in different axial distance of the channels.

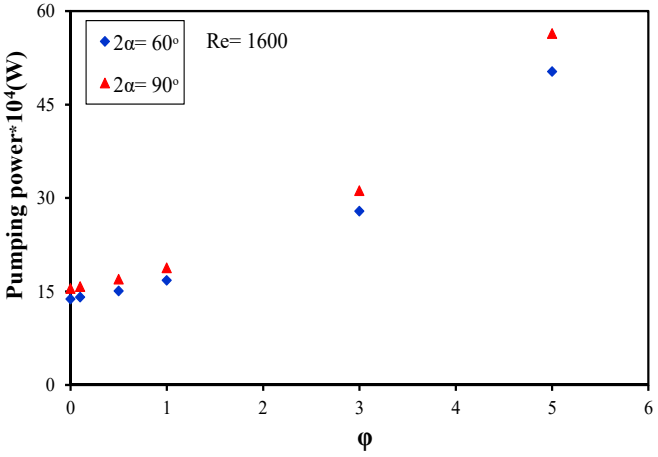

Fig. 11. Pumping power of fluids vs. nanoparticle concentration in the two apex angles.

7. Conclusions

In the present study laminar convection heat transfer of Al_2O_3/water nanofluids flowing through horizontal isosceles triangular ducts subjected to constant wall heat flux was studied numerically. Simulations were carried out according to the single-phase model. It was found that by increasing the distance from the duct inlet, the local heat transfer coefficients of nanofluids decreases. Both the local heat transfer coefficient and the Nusselt number of nanofluids was enhanced by increasing the nanoparticle concentration. The enhancement of both the local heat transfer coefficient and the Nusselt number of nanofluids were larger at the entrance of the ducts. As expected, the average Nusselt number of nanofluids increased by increasing the Peclet number. The effect of the Peclet number on the enhancement of nanofluids heat transfer is larger for ducts with a higher apex angle. Results show that the average heat transfer coefficient and the Nusselt number of nanofluids are higher than that of the base fluid and increase by increasing the nanoparticle concentration. The enhancement of the heat transfer coefficient is much higher than that of the Nusselt number. Results also show that the influence of nanoparticles on the heat transfer enhancement of nanofluids is almost independent of the apex angle of the channels. Results show that $f_{app}Re$ decreases by increasing the axial distance from the inlet of channels and approaches a constant value in the fully developed region. Velocity profiles of fluids on a symmetry plane exhibit two local maximums near the inlet of the channels, their positions are independent of nanofluids concentration but their values are affected by nanofluid concentration. The velocity profiles of fluids reaches a maximum in the fully developed region where its position is the same for all fluids, but its magnitude increases when the nanoparticle concentration increases. The required pumping power in channels with an apex angle of 60° is less than that of channels with an apex angle of 90°. Overall, it seems that the channel with an apex angle of 60° is more convenient.

Nomenclature

C_p: Heat capacity (kJ/kgK)
D_h: Duct hydraulic diameter (m)
f: Darcy friction factor (dimensionless)
h: Average heat transfer coefficient (W/m^{2}K)
h_z: Local heat transfer coefficient (W/m^{2}K)
k: Thermal conductivity (W/m K)
l: Hydrodynamic entrance length (m)
L: Length of channel (m)
L^+: Dimensionless hydrodynamic entrance length (dimensionless)
$\dot{m}$: Mass flow rate (kg/s)
N: Number of nodes (dimensionless)
Nu: Average Nusselt number (dimensionless)
p: Pressure (kPa)
T: Temperature (K)
V: Fluid velocity (m/s)
$\dot{W}$: Power (J)
z: Axial distance from duct inlet (m)
z*: Dimensionless hydrothermal distance from duct inlet (= zD_h / RePr)
z^+: Dimensionless hydrodynamic distance from duct inlet (= z / D_hRe)

Greek symbols

α: Half-apex angle of triangular duct (degrees)
φ: Particle volume percent (dimensionless)
ρ: Density (kg/m^3)
μ: Fluid viscosity (Pa.s)

Subscript

app: apparent
bf: base fluid
eff: effective
nf: nanofluid
np: nanoparticle
p: particle
pump: pump

References

[1] J.C. Maxwell, A Treatise on Electricity and Magnetism, 2nd ed., Clarendon Press, Oxford, UK, 1881.
[2] R. Lotfi, Y. Saboohi, A.M. Rashidi, Numerical study of forced convective heat transfer of nanofluids: Comparison of different approaches, Int. Commun. Heat Mass, 37 (2010) 74-78.
[3] M. Saberi, M. Kalbasi, A. Alipourzade, Numerical study of forced convective heat transfer of nanofluids inside a vertical tube, Int. J. Therm. Technol. 3 (2013)

10-15.

[4] V. Bianco, O. Manca, S. Nardini, Numerical Simulation of water/Al_2O_3 nanofluid turbulent convection, Adv. Mech. Eng. 2 (2010) Article ID 976254.

[5] V. Bianco, O. Manca, S. Nardini, Numerical investigation on nanofluids turbulent convection heat transfer inside a circular tube, Int. J. Therm. Sci. 50 (2011) 341-349.

[6] M. Nazififard, M. Nematollahi, K. Jafarpur, K.Y. Suh, Numerical simulation of water-based alumina nanofluid in subchannel geometry, Sci. Technol. Nucl. Ins. 2012 (2012) Article ID 928406.

[7] M. Rostamani, S.F. Hosseinizadeh, M. Gorji, J.M. Khodadadi, Numerical study of turbulent forced convection flow of nanofluids in a long horizontal duct considering variable properties, Int. Commun. Heat Mass, 37 (2010) 1426-1431.

[8] M.R. Ghavam, M. Hojjat, S.G. Etemad, Numerical investigation on forced convection heat transfer of nanofluids through isosceles triangular ducts, in: Proceedings of the 3rd International Conference on Nanotechnology: Fundamentals and Applications, Montreal, Quebec, Canada, 2012.

[9] E. Ebrahimnia-Bajestan, H. Niazmand, W. Duangthongsuk, S. Wongwises, Numerical investigation of effective parameters in convective heat transfer of nanofluids flowing under a laminar flow regime, Int. J. Heat Mass Tran. 54 (2011) 4376-4388.

[10] S. Mirmasoumi, A. Behzadmehr, Numerical study of laminar mixed convection of a nanofluid in a horizontal tube using two-phase mixture model, Appl. Therm. Eng. 28 (2008) 717-727.

[11] P.K. Namburu, D.K. Das, K.M. Tanguturi, R.S. Vajjha, Numerical study of turbulent flow and heat transfer characteristics of nanofluids considering variable properties, Int. J. Therm. Sci. 48 (2009) 290-302.

[12] S.E.B. maïga, C.T. Nguyen, N. Galanis, G. Roy, Heat transfer behaviours of nanofluids in a uniformly heated tube, Superlattice. Microst. 35 (2004) 543-557.

[13] S.E.B. Maïga, S.J. Palm, C.T. Nguyen, G. Roy, N. Galanis, Heat transfer enhancement by using nanofluids in forced convection flows, Int. J. Heat Fluid Fl. 26 (2005) 530-546.

[14] S. Tahir, M. Mital, Numerical investigation of laminar nanofluid developing flow and heat transfer in a circular channel, Appl. Therm. Eng. 39 (2012) 8-14.

[15] M. Nuim Labib, M.J. Nine, H. Afrianto, H. Chung, H. Jeong, Numerical investigation on effect of base fluids and hybrid nanofluid in forced convective heat transfer, Int. J. Therm. Sci. 71 (2013) 163-171.

[16] A. Azari, M. Kalbasi, M. Rahimi, CFD and experimental investigation on the heat transfer characteristics of alumina nanofluids under the laminar flow regime, Braz. J. Chem. Eng. 31 (2014) 469-481.

[17] M. Izadi, A. Behzadmehr, D. Jalali-Vahida, Numerical study of developing laminar forced convection of a nanofluid in an annulus, Int. J. Therm. Sci. 48 (2009) 2119-2129.

[18] M. Shariat, A. Akbarinia, A.H. Nezhad, A. Behzadmehr, R. Laur, Numerical study of two phase laminar mixed convection nanofluid in elliptic ducts, Appl. Therm. Eng. 31 (2011) 2348-2359.

[19] S.G. Etemad, M. Hojjat, J. Thibault, J.B. Haelssig, Heat transfer of nanofluids through a Square channel: A numerical study, in: Proceedings of the International Conference on Nanotechnology: Fundamentals and Applications, Ottawa, Ontario, Canada, 2010.

[20] S. Zeinali Heris, A. Kazemi-Beydokhti, S.H. Noie, S. Rezvan, Numerical Study on Convective Heat Transfer of Al_2O_3/Water, CuO/Water and Cu/Water Nanofluids through Square Cross-Section Duct in Laminar Flow, Eng. Appl. Comp. Fluid, 6 (2012) 1-14.

[21] P.R. Mashaei, S.M. Hosseinalipour, M.B.M. Dirani, 3-D Numerical simulation of nanofluid laminar forced convection in a channel with localized heating, Aust. J. Bas. Appl. Sci. 6 (2012) 479-489.

[22] M.K. Abdolbaqi, C.S.N. Azwadi, R. Mamat, Heat transfer augmentation in the straight channel by using nanofluids, Case Stud. Therm. Eng. 3 (2014) 59-67.

[23] S.Z. Heris, F. Oghazian, M. Khademi, E. Saeedi, Simulation of convective heat transfer and pressure drop in laminar flow of Al_2O_3/water and CuO/water nanofluids through square and triangular cross-sectional ducts, J. Renew. Energ. Environ. 2 (2015) 6-18.

[24] T. Nassan, S. Zeinali Heris, S.H. Noie Baghban, A comparison of experimental heat transfer characteristics for Al_2O_3/water and CuO/water nanofluids in square cross-section duct, Int. Commun.

Heat Mass, 37 (2010) 924-928.

[25] B. Mehrjou, S.Z. Heris, K. Mohamadifard, Experimental study of CuO/Water nanofluid turbulent convective heat transfer in square cross-section duct, Exp. Heat Transfer, 28 (2015) 282-297.

[26] R.-Y. Jou, S.-C. Tzeng, Numerical research of nature convective heat transfer enhancement filled with nanofluids in rectangular enclosures, Int. Commun. Heat Mass, 33 (2006) 727-736.

[27] S. Zeinali Heris, S.H. Noie, E. Talaii, J. Sargolzaei, Numerical investigation of Al_2O_3/water nanofluid laminar convective heat transfer through triangular ducts, Nanoscale Res. Lett. 6 (2011) 179.

[28] H.E. Ahmed, M.I. Ahmed, M.Z. Yusoff, Heat transfer enhancement in a triangular duct using compound nanofluids and turbulators, Appl. Therm. Eng. 91 (2015) 191-201.

[29] H.E. Ahmed, M.Z. Yusoff, M.N.A. Hawlader, M.I. Ahmed, B.H. Salman, A.S. Kerbeet, Turbulent heat transfer and nanofluid flow in a triangular duct with vortex generators, Int. J. Heat Mass Tran. 105 (2017) 495-504.

[30] S.Z. Heris, Z. Edalati, S.H. Noie, O. Mahian, Experimental investigation of Al_2O_3/water nanofluid through equilateral triangular duct with constant wall heat flux in laminar flow, Heat Transfer Eng. 35 (2014) 1173-1182.

[31] S.Z. Heris, F. Ahmadi, O. Mahian, Pressure drop and performance characteristics of water-based Al_2O_3 and CuO nanofluids in a triangular duct, J. Disper. Sci. Technol. 34 (2013) 1368-1375.

[32] B.C. Pak, Y.I. Cho, Hydrodynamic and heat transfer study of dispersed fluids with submicron metallic oxide particles, Exp. Heat Transfer, 11 (1998) 151-170.

[33] R.K. Shah, A.L. London, Laminar Flow Forced Convection in Ducts, Academic Press, New York, 1978.

[34] S.G. Etemad, Laminar Heat transfer to viscous non-Newtonian fluids in non-circular ducts, McGill University, Montreal, Quebec, Canada, 1995.

[35] S.G. Etemad, A.S. Mujumdar, R. Nassef, Simultaneously developing flow and heat transfer of non-Newtonian fluids in equilateral triangular duct, Appl. Math. Model. 20 (1996) 898-908.

[36] Y.A. Çengel, J.M. Cimbala, Fluid Mechanics: Fundamentals and Applications, McGraw-Hill Higher Education, Boston, 2006.